Studying the Effect of Different Etching Parameters on the Physical Properties of Porous Silicon Prepared By Electrochemical Etching

Dr. Uday Muhsin Nayef
Applied Science Department, University of Technology/Baghdad.
Haider Amer Khalaf
Applied Science Department, University of Technology/Baghdad.
Email: haider14ak@gmail.com

Revised on:15/3/2015 & Accepted on:11/6/2015

ABSTRACT:

In this work we prepared a porous Silicon (PS) layer by electrochemical etching (ECE) technique using different etching parameters including current density, anodization time and Hydrofluoric (HF) acid concentration. From the structural properties, we found that the full width half maximum of the observed spectrum from the XRD analysis has been increased and the peak position is slightly shifted to higher value. Also the etching parameters effect on the pore diameter and in turn on all chemical compositional and optical properties. As well as for electrical properties, the barrier height increases with pore diameter and the depletion width as well. From these result, it can tell that PS layer is better than c-Si for many applications.
Keyword: Porous Silicon, electrochemical etching, physical properties

دراسة تأثير عوامل التنميش المختلفة على الخصائص الفيزيائية لمادة السليكون المسامي المحضر بطريقة التنميش الكهروكيميائي

الخلاصة:

في هذا البحث حضرنا طبقة من السليكون المنمش بواسطة تقنية التنميش الكهروكيميائية مستخدمين مختلف عوامل التنميش من ضمنها كثافة تيار التضمين و زمن التنميش و تركيز حامض الهيدروفلوريك. من الخصائص التركيبية وجدنا ان هناك توسع ملحوظ في طيف حيود الأشعة السينية مع انحراف القمة عن موقعها الأصلي. كذلك عوامل التنميش تؤثر على قطر التجويف و التي بدورها تؤثر على خصائص التركيب الكيميائي و الخواص البصرية. و في الخصائص لكهربائية يزداد ارتفاع حاجز الجهد مع مع قطر التجويف و عرض منطقة النضوب. و من هذه النتائج نستنتج ان الطبقة المتكونة بعد عملية التنميش تمتلك خصائص افضل من السليكون البلوري و تستخدم في العديد من التطبيقات.

INTRODUCTION

Porous Silicon (PS) has been intensively studied by many researchers due to its unique properties that used for many optoelectronic applications including Light emitting diode and photo-detector [1]. PS represents as a Nanostructure Silicon (Si) that has larger band-gap with respect to the crystalline Silicon (c-Si) which appears as sponge-like structure with pores separated by Nano-sized walls [2]. Depending on the pore sizes, the PS can be divided into three types: Micro-porous,

https://doi.org/10.30684/etj.2015.116734
2412-0758/University of Technology-Iraq, Baghdad, Iraq

Meso-porous and Macro-porous with sizes less < 2, 2 - 50 and > 50 nm respectively [3]. The most parameters that affect the porosity, etching rate, and electro-polishing threshold (or critical current) are etching current density, etching time, and Hydrofluoric (HF) acid. The main goal of this research is to get the desired physical characteristics which can be easily obtained by controlling the mentioned parameters

Experimental Work

A PS layer is the result of a complicated balance of processes that occur during electrochemical etching (ECE) which is the most common methods including the dissolution of Si wafers in hydrofluoric acid (HF) solutions. The typical schematic diagrams of PS setup are shown in Fig. 1 which are generally used. The cell body is usually made of highly acid-resistant polymer such as polytetrafluoroethylene "Teflon" (PTFE). The backside of the Si after attached with an Aluminum contact is placed on a metal disk and sealed with an O-ring on the front side where the wafer surface exposed to HF. The pore growth starts after applying a voltage between the Si wafer (the anode) and a circular grid usually made from gold or platinum (the cathode).

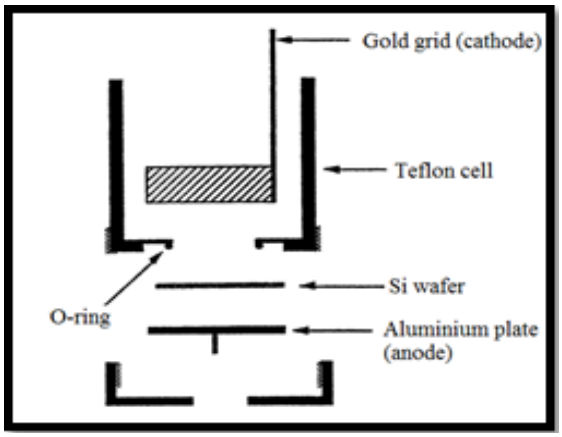

Figure(1): Cross-sectional view of a single-tank anodization electrochemical cell

During the reaction, Hydrogen bubbles is created on the Si surface where can effect negatively on the homogeneity and the uniformity of the PS layer. This problem can be solved by dilute the used acid with ethanol [4]. Finally, the PS layer is rinsed with pentane and ethanol and then dried. The following equations that used in this work are [5-6]:

$$\eta = \left(\frac{q}{K_B T}\right)\left(\frac{dV}{d(\ln I)}\right) \quad \ldots(1)$$

$$J_o = A^* T^2 \exp\left(\frac{-q\Phi_B}{K_B T}\right) \quad \ldots(2)$$

$$\Phi_B = \frac{K_B T}{q} \ln\left(\frac{A^* T^2}{J_o}\right) \quad \ldots(3)$$

$$N_A = \frac{2}{q\varepsilon_{si}\xi^2}\left(\frac{dC^{-2}}{dV}\right)^{-1} \quad \ldots(4)$$

$$\Phi_B = \frac{qN_A W^2}{2\varepsilon_{si}} \quad \ldots(5)$$

Where
η is the ideality factor, K_B is Boltzmann's constant ($1.38*10^{-23}$ J/K), J_o is the saturation current, A^* is the effective Richardson constant (32 A/cm^{2}K^2 for p-type Si), Φ_B is the zero-bias barrier height, ε_{si} is semiconductor permittivity (11.7 x 1.04 x 10^{-12} F/cm), ξ is a factor depending on the carrier concentration of silicon substrate (0.2) and dV/dC^2 is the slope.

Results and Discussions

Structural Properties

The structural properties of PS have been analyzed using X-ray diffraction (XRD) technique. XRD spectra of PS exhibit broadening and slightly shift to higher diffraction angle (2θ = 28.56°) than the bulk Si peak (2θ = 28.44°) according to (JCPDS: 27-1402) as shown in Fig. 2. The changing in FWHM between Si and PS can be explained in which the crystalline atoms of PS cause a beam of X-rays to diffract from the walls between pores into many specific directions and the structure remains crystalline but in Nano-Sized [7]. Also the deviation is attributed to the oxide layer formed on the surface of the PS layer as reported by Weiss et.al (2003) [8].

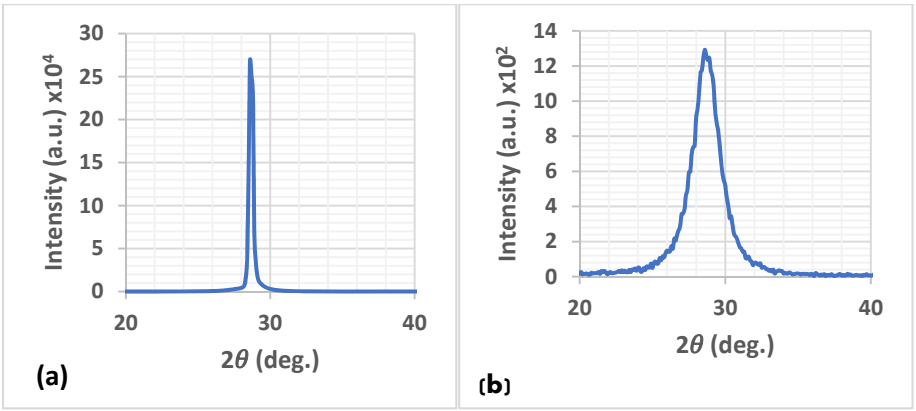

Figure(2): XRD spectra of (a) c-Si and (b) PS prepared at current density (30 mA/cm^2) with fixed etching time and HF concentration (20 min and 15 % respectively).

The Raman spectra in Fig. 3 represents for bulk and PS with current density (30 mA/cm^2) in the range from (500-550 cm^{-1}). From the figure it is found that the PS slightly shift towards lower energy. This might be attributed to morphological structure as the surface roughness decrease intensively. The Raman intensity from PS is about 10 times stronger than that from c-Si which is due to optical phonon confinement in the PS sample which has an agreement with Ali et.al (2009) [9].

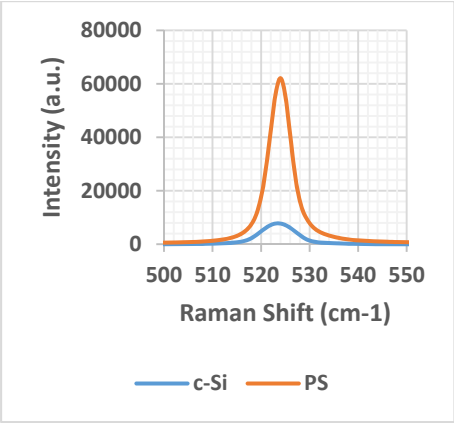

Figure(3): A compression of Raman spectra between c-Si and PS.

Morphological Properties

The morphological properties have been analyzed using an atomic force microscope (AFM) instrument taking images in the Nano-metric scale. Table 1 shows the morphological characteristics calculation of PS including average diameter (D_a), average roughness (R_a) and root mean square (RMS) at different current density (J), etching time (t) and HF concentration (HFc) which has been estimated from Fig. 4. As noticed, the value of pore size increases with current density, etching time and HF concentration due to the silicon dissolution process within the PS layer that comes from an increasing in the etching rate, during time or more Fluoride ions that supplied by HF respectively. Further, the pore diameter decreases due to chemical dissolution making pores to immerge together until completely dissolved and new growth of pores for new layer is occurs. These results have an agreement with Kim et al. (2003), Asli et al. (2011) and Kumar et.al (2011) [10-12].

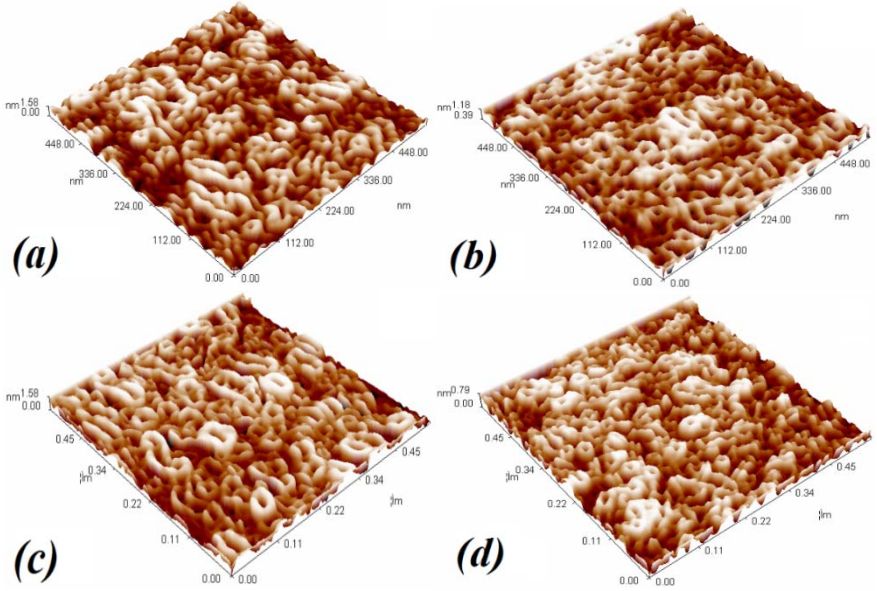

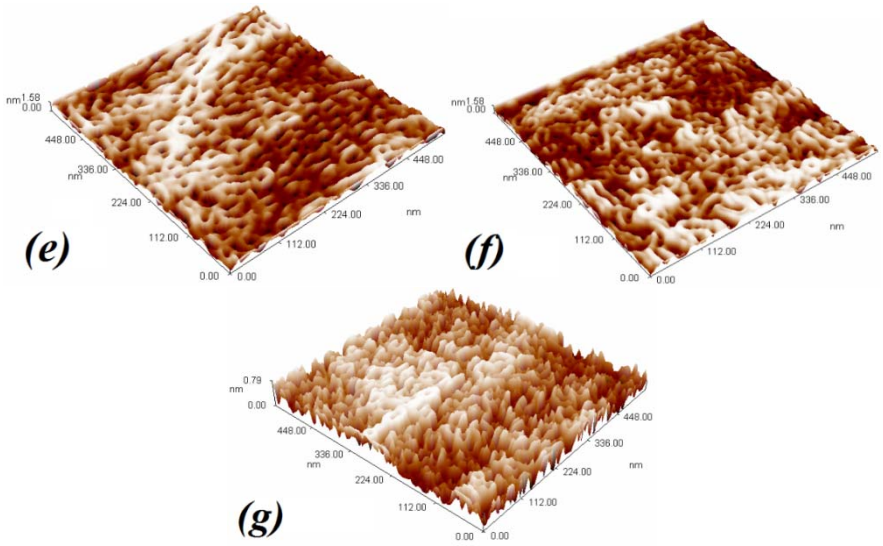

Figure(4): 3D AFM images of PS samples for different etching parameters (*a*) 10, (*b*) 30, (c) 40 and (d) 50 mA/cm^2, (*e*) 5 and (*f*) 30 min and (*g*) 30 %.

Moreover, the average roughness and RMS are changed according to the size of pore diameter. The average pore diameter seems to have irregular sizes and range between (15.95 – 30.53 nm) leaves PS layer to be in a good agreement for a Meso-porous layer.

Table(1): morphological characteristics calculation of PS samples at different etching parameters (paras.).

Etching Paras.	Fixed Paras.	D_a (nm)	R_a (nm)	RMS (nm)
J (mA/cm^2)				
20	t = 20 min , HFc = 15 %	15.95	0.371	0.429
30		24.38	0.186	0.216
40		30.53	0.364	0.424
50		19.95	0.182	0.212
t (min)				
5	J = 30 mA/cm^2 , HFc = 15 %	18.48	0.374	0.435
30		21.92	0.373	0.433
HFc (%)				
25	J = 30 mA/cm^2 , t = 20 min	16.93	0.173	0.203

Compositional Properties

Chemical bonds for determining the reaction occurs in PS after etching bond can be analyzed using Fourier Transform Infrared (FTIR) spectroscopy which presented as a non-destructive analytical tool. The peak of absorption IR and chemical bonds are compared with other references as listed in table 2. PS has a large initial surface area allowing the existence of enormous quantities of impurities that come from the electrolyte used for electro chemical etching (ECE) and from the ambient air [13]. The oxidation level of PS is very important in physical properties. The main peaks of Si-H and Si-O groups are taken into account. As the pore diameter increases, the Si-Si bonds (611 cm^{-1}) decreases as it interacts with Oxygen and Hydrogen atoms and other contamination (see Fig. 5).

Table (2): peaks position compression for c-Si (S1) and PS with different current densities 20 (S2) and 30 (S3) mA/cm^2 [14-17].

Peak Ref.	S1 peak	S2 peak	S3 peak	Bonds
(cm^{-1})				
611	611	611	605	Si-Si
662	681	662	659	Si-H_2 Roll
720	730	727	739	Si-F
799	785	789	790	SiO-H Stretch
810	-	818	829	C-H Bend
860	-	860	865	Si-H_2 Wag
880	872	890	893	Si-O-Si Bend
937	-	933	930	Si-H_3 Bend
980	983	979	975	SiH Bend
1080	-	1008 to 1244	1102 to 1255	Si-O-Si symmetric stretch
1105				
1150				
1250				
1400	-	1370	1376	CH_3 symmetric stretch

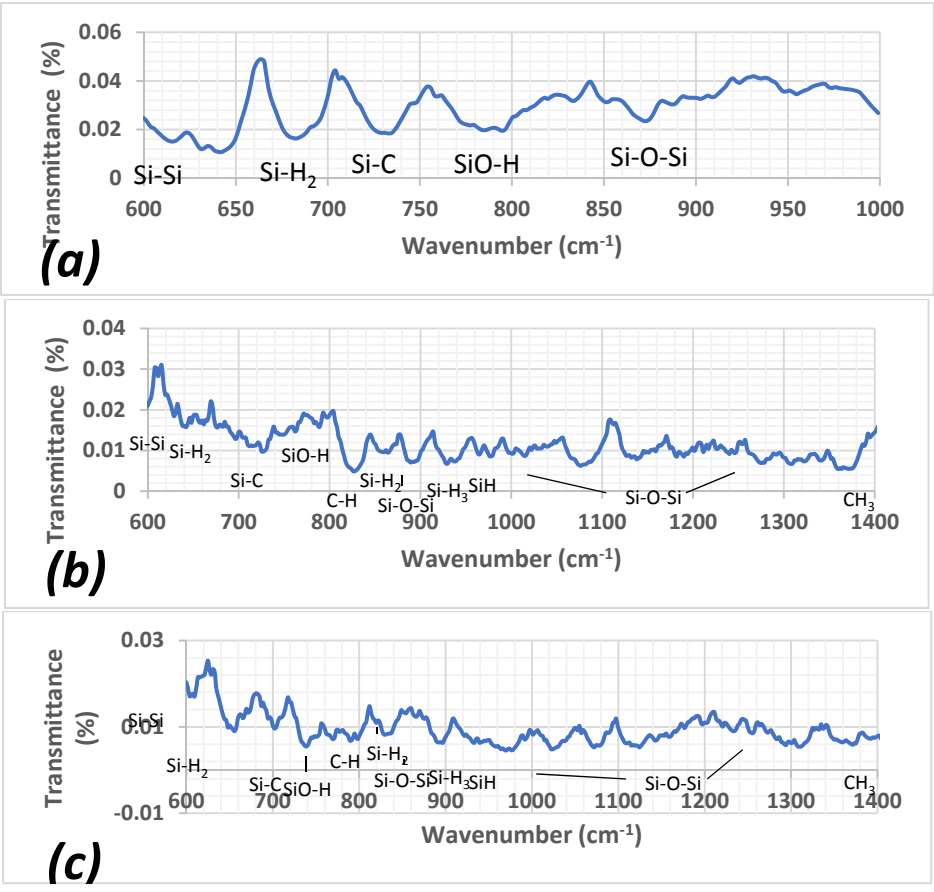

Figure(5): FTIR absorption spectra of (a) bulk Si (111) and PS for different current densities (b) 20 and (c) 30 mA/cm^2 fixed etching time and HF concentration

Optical Properties

One of most intensive study in optical properties of PS is the reflectivity as it depends strongly on the surface morphology. The high degree of roughness and increasing porosity are the mine parameters that reduce the reflection of light as reported by Pap et al. (2006) [18]. The formed thin layer of PS cause the photons of light to be scattered and trapped inside the structure where the scattering of light is may be due to the surface roughness at the PS/Si interface which attribute to the changing in refractive index while the trapping is due to total internal reflection within the porous layer by increasing the optical path length hence increase the absorption by the Silicon structure [19]. According to Fig. 6 where the reflectance spectra of c-Si has the most reflectivity than PS samples, some samples has a sine wave curve which may be attributed to a multilayer formation [20].

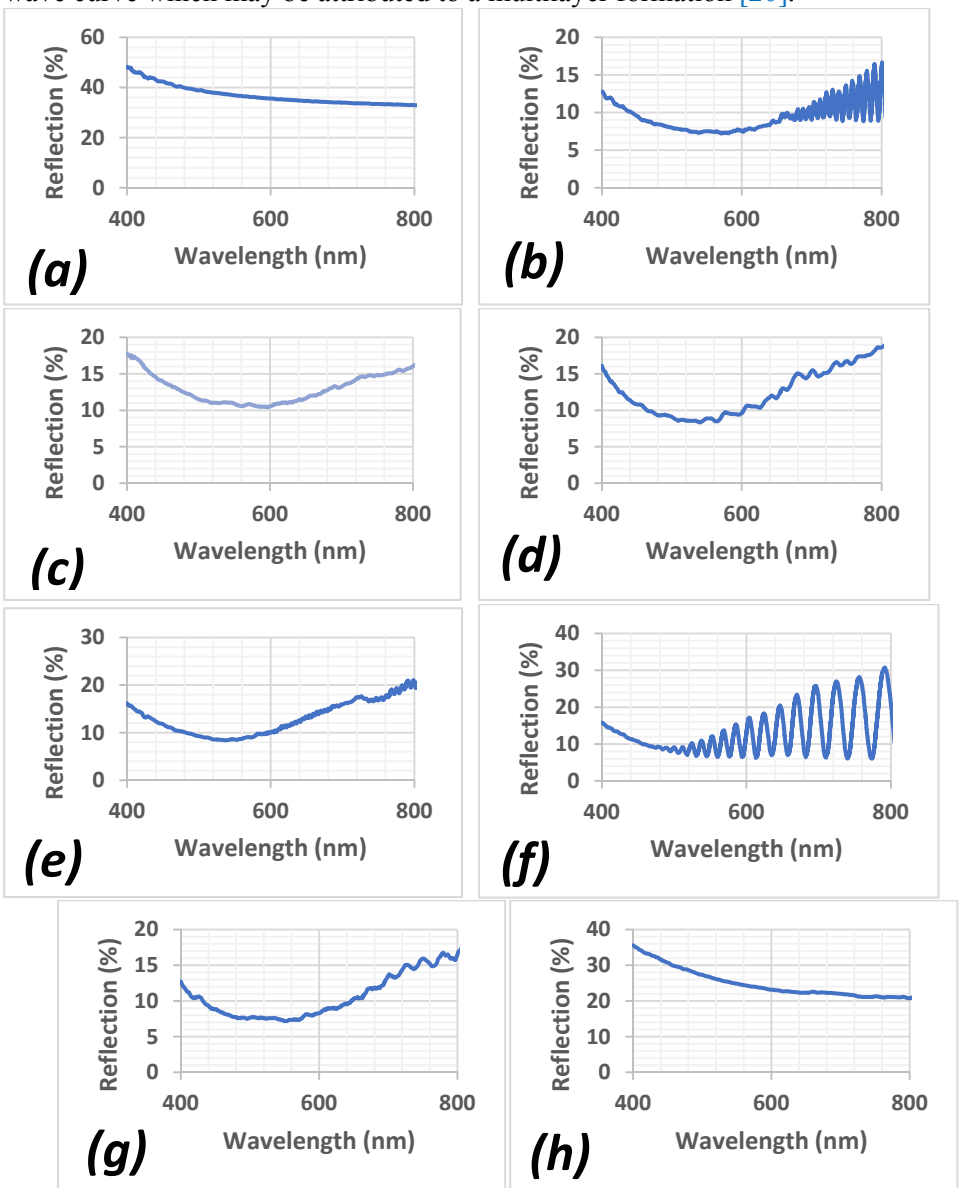

Figure(6): The reflection spectra of (a) c-Si and PS using different conditions (b) 20, (c) 30, (d) 40 and (e) 50 mA/cm^2, (f) 5 and (g) 30 min and (h) 25 %.

Electrical Properties

The electrical measurements involve the study of current density - Voltage (J-V) and current density - capacitance (C-V) characteristics. The hetero-structure between c-Si and PS in form of Al/PS/c-Si/Al has been studied for different etching parameters. The J-V measurements were achieved in dark surround and under illumination at room temperature. Fig. 7 shows rectifying behavior between two biases (forward and reverse) which could be attributed to the formation of a junction like isotope hetero-junction [21]. This behavior described by the differences in their energy band-gap, which has been described by quantum confinement effect (QCE), as it is an important to explain the increasment of resistivity for PS/c-Si hetero-structure.In result, the output current vary as the structure size change [22]. Table (3) shows the saturation current density (J_S) which has been determined from the log-linear region of the current density to zero voltage, the ideality factor (η) and barrier height (Φ_B).

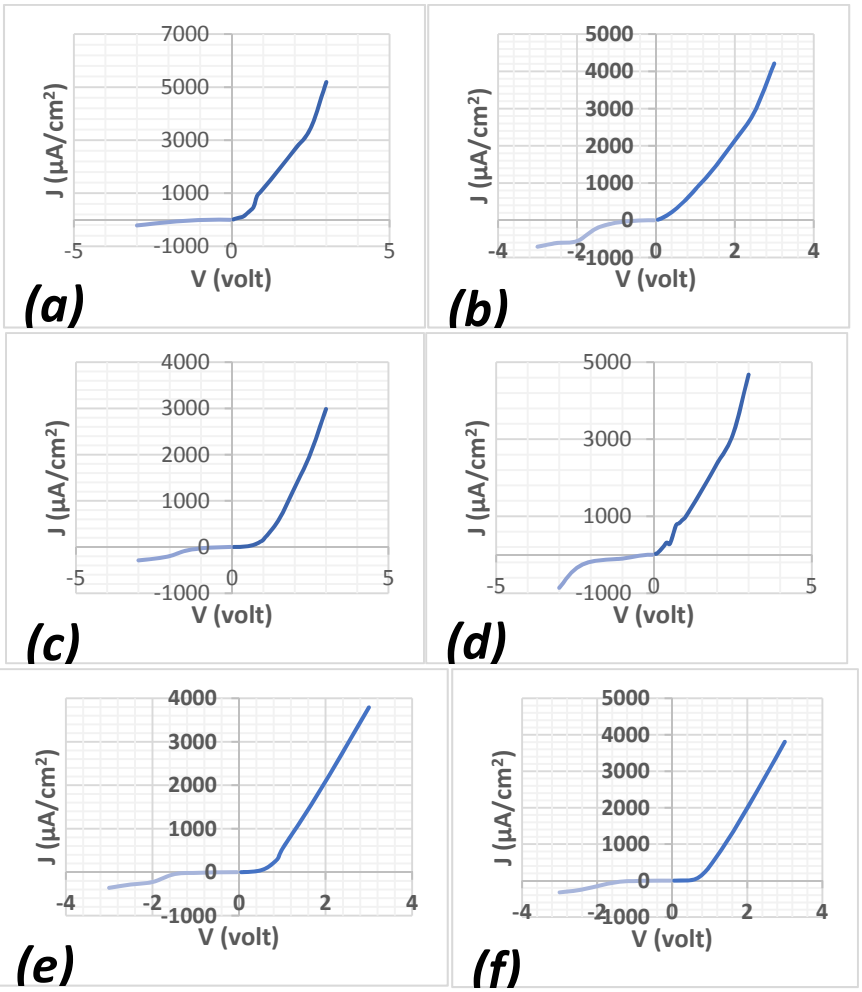

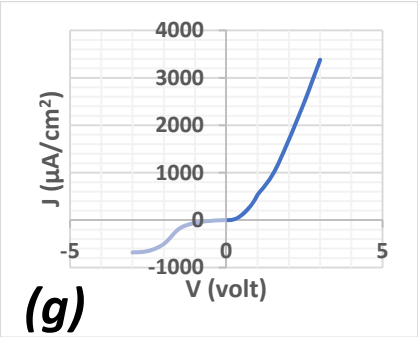

Figure (7): *J-V* characteristics of Al/PS/p-Si/Al different etching parameters (*a*) 10, (*b*) 30, (c) 40 and (d) 50 mA/cm^2, (*e*) 5 and (*f*) 30 min and (*g*) 30 %.

The high value of the obtained ideality factor, which is higher than for an ideal diode, can be explained by the formation of high density of states at the interface between c-Si and PS which acts as recombination centers in the PS layer [23].

Table (3): shows *J-V* characteristics of PS at different etching parameters.

Etching Para.	Fixed Paras.	J_S (μA)	η	Φ_B (eV)
J (mA/cm^2)				
20	t = 20 min , HFc = 15 %	900	2.83	0.566
30		740	3.11	0.571
40		470	3.89	0.583
50		770	2.95	0.570
t (min)				
5	J = 30 mA/cm^2 , HFc = 15 %	880	3.12	0.567
30		600	3.26	0.577
HFc (%)				
25	J = 30 mA/cm^2 , t = 20 min	660	3.21	0.574

Studying photo-current for PS is an important due to the effect of light on photo-sensitivity, and generally on detection properties. Taking the reverse bias instead of forward is because of depletion layer raise in revers bias and clearly show the photon generation effect of electrons-holes pairs as it is increases with the applied incident power density, while for forward bias the depletion layer will reduced hence lead to no effect of light leaving current to be limited by the resistance of PS layer. Fig. 8 shows the J-V characteristics of two PS samples with different etching current densities, for comparison, using different power intensities (5, 20, 60 and 125 mW/cm^2) at room temperature. The more power applied, higher output current can achieved due to the increasing in the number of the generated photo carriers which has an agreement with Nathera et al. (2012) [24]. The overall output currents are decreases when the band-gap increasing for the same light power applied.

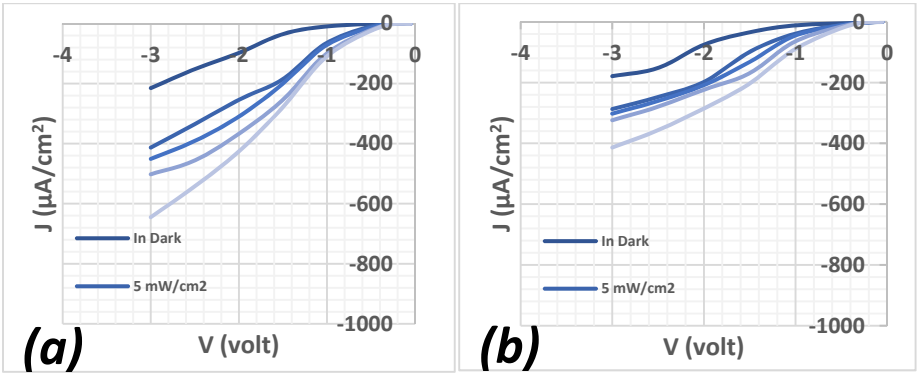

Figure(8): photo-current of Al/PS/c-Si/Al for revers bias under dark and illumination, prepared with different current densities (a) 20 and (b) 40 mA/cm^2.

Semiconductor materials, in general, have an empty region called a depletion region. This region affected by the applied voltage and act as capacitor. By measuring the capacitance and take the reciprocal of its square ($1/C^2$) versus the applied voltage (V) the built-up potential (Φ_B) can be determined and the carrier's concentration (N_A) and depletion width layers (W) can be estimated using equations 4 and 5 where these variables are listed in table 4. Fig. 9 and Fig. 10 show the C-V characteristics and Φ_B calculation plot, respectively, of PS samples with the same etching parameters that mentioned in the J-V measurement. As the current density, etching time or HF concentration increase, the capacitance of the PS layer increase and this attributed to the increasing in the depletion width which leading to the increasing in barrier height [25].

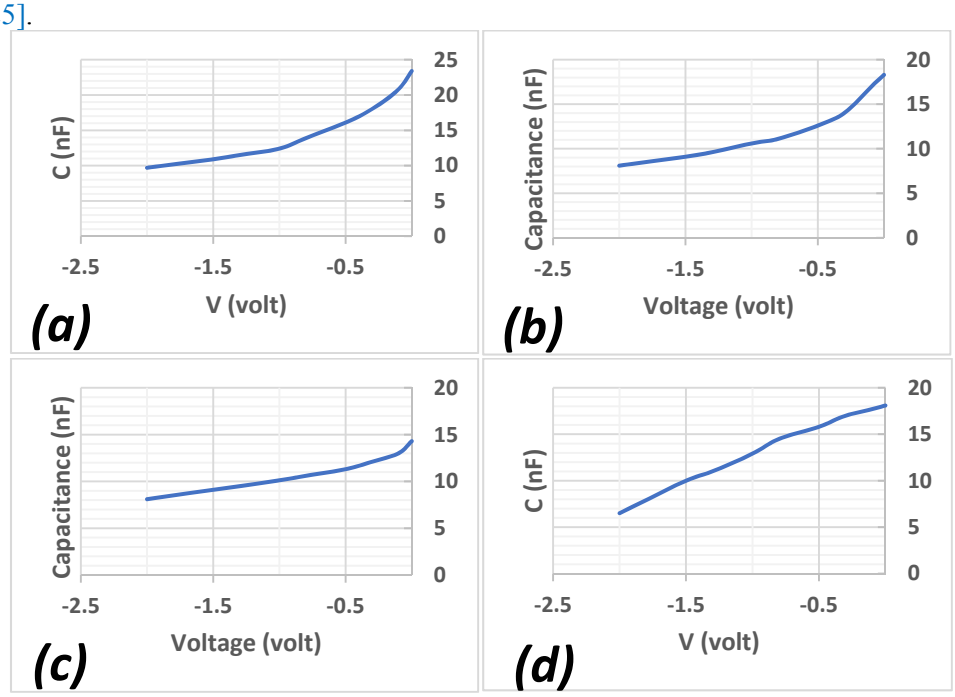

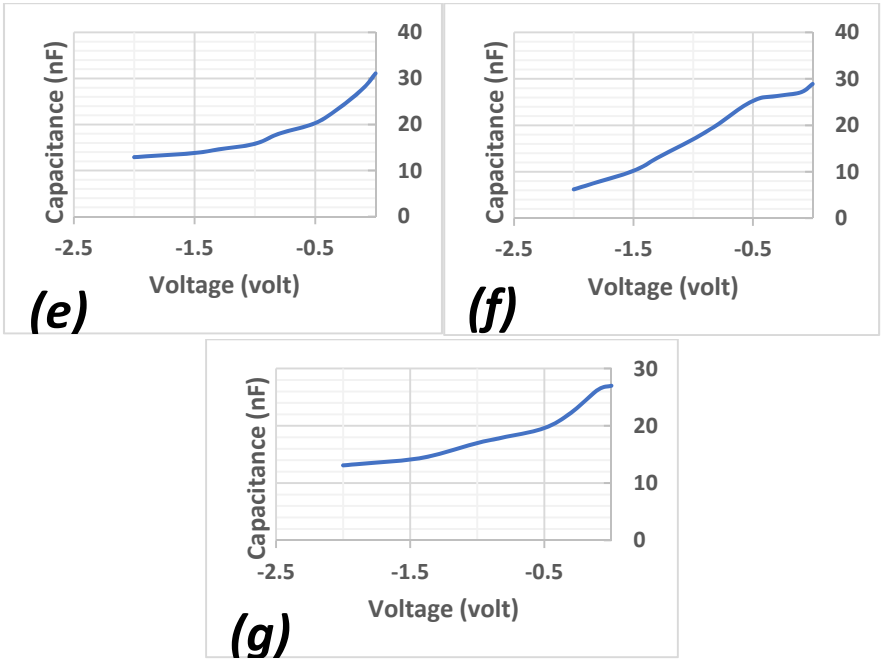

Figure(9): C-*V* characteristics of Al/PS/p-Si/Al at different etching parameters (*a*) 10, (*b*) 30, (c) 40 and (d) 50 mA/cm^2, (*e*) 5 and (*f*) 30 min and (*g*) 30 %.

The ($1/C^2$) versus (V) could be useful to know wither the depletion layer is constant or not where if the result give a straight then "abrupt" then the layer is constant and the distribution of the carrier concentrations are homogeneous. Otherwise, if the line is curved "gradient" then the layer is not constant and the carrier concentrations are distributed unequally [26].

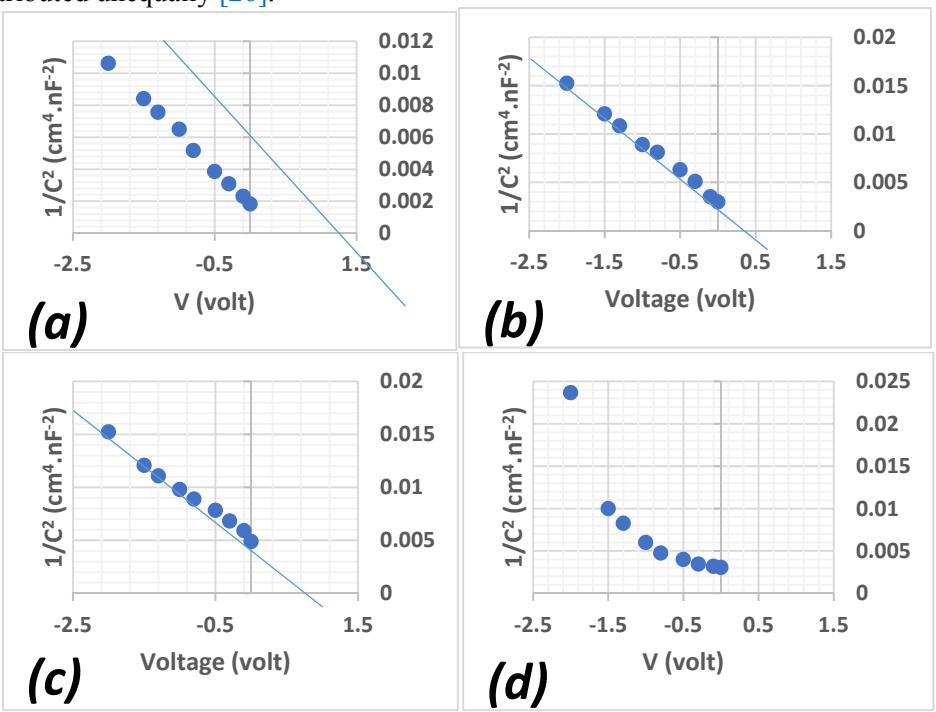

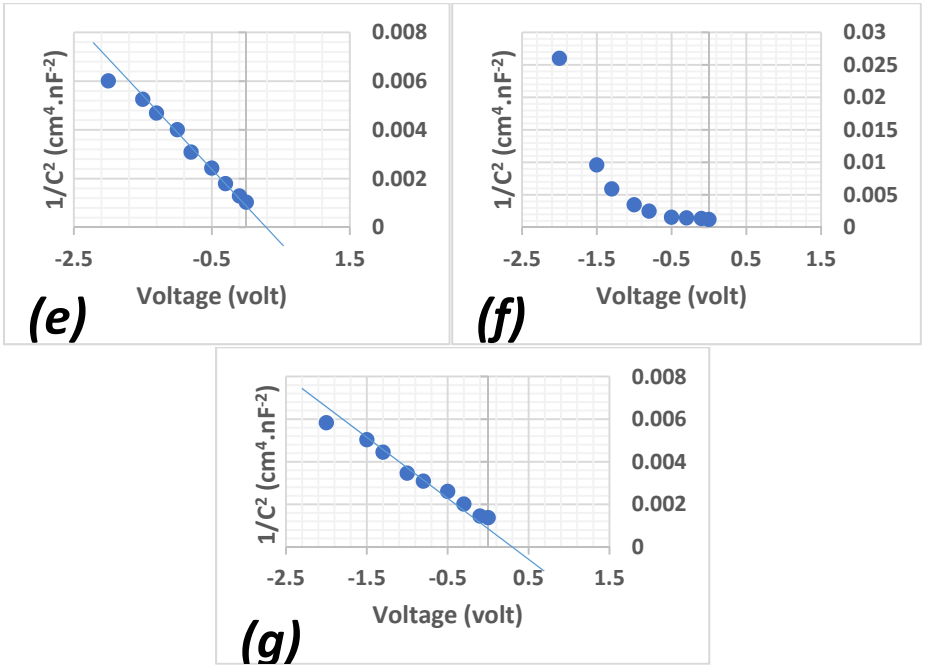

Figure(10): voltage vs. $1/C^2$ of Al/PS/p-Si/Al different etching parameters (*a*) 10, (*b*) 30, (c) 40 and (d) 50 mA/cm^2, (*e*) 5 and (*f*) 30 min and (*g*) 30 %.

Table (4): shows *C-V* characteristics of PS at different etching parameters.

Etching Para.	Fixed Paras.	N_A (cm^{-3}) x10^{15}	W (µm)	Φ_B (V)
J (mA/cm^2)				
20	t = 20 min , HFc = 15 %	7.5	0.91	0.41
30		8.2	0.99	0.53
40		8.7	1.11	0.62
50		-	-	-
t (min)				
5	J = 30 mA/cm^2 , HFc = 15 %	7.5	0.91	0.41
30		-	-	-
HFc (%)				
25	J = 30 mA/cm^2 , t = 20 min	8.4	1.01	0.57

CONCLUSION

From the analysis we can conclude that the pore diameter of the PS films increases with current density, etching time and HF concentration which can give best results for a certain value where an electro-polishing can occur for further increment and lead to uncontrollable process. However, the PS films give an enhanced results comparing to c-Si and it is good for optoelectronic applications.

REFERENCES

[1] Charrier J, Le Gorju E, Haji L, et al. Optical Waveguides Fabricated from Oxidised Porous Silicon. J Porous Materials. (2000);7(1-3):243-246.

[2] Salman KA, Hassan Z, Omar K. Effect of Silicon Porosity on Solar Cell Efficiency. Int. J Electrochemical Science. (2012);7(1):376-386.
[3] Fan D. Mesoporous Silicon Biopolymer Composites for Orthopedic Tissue Engineering and Drug Delivery Applications [Dissertation]. Beijing (CN): Beijing Normal University; 2008. 194 p.
[4] Dubey RS. Electrochemical Fabrication of Porous Silicon Structures for Solar Cells. J Nanoscience and Nanoengineering. (2013);1(1):36-40.
[5] El-Zohary SE, Shenashen MA, Allam NK, et al. Electrical Characterization of Nanopolyaniline/Porous Silicon Heterojunction at High Temperatures. J Nanomaterials. (2013);2013:8p.
[6] Pineik E, Jergel M, Bartos J, et al. The C-V investigation of light-related properties of porous siliconcrystalline silicon structure. [J Surfaces and vacuum]. 1999;9:78-81. Spanish.
[7] Jayachandran M, Paramasivam M, Murali KR, et al. Synthesis of Porous Silicon Nanostructure for Photoluminescent Devices. Materials Physics and Mechanics. (2001);4(2):143-147.
[8] Weiss SM, Molinari M, Fauchet PM. Temperature stability for silicon-based photonic band-gap structures. Applied Physics Letters. (2003);83(10):1980-1982.
[9] Ali NK, Hashim MR, Abdul Aziz A. Pulse Current Electrochemical Deposition of Silicon for Porous Silicon Capping to Improve Hardness and Stability. Electrochemical and Solid-State Letters. (2009);12(3):D11-D14.
[10] Kim DA, Lee JS, Park MB, et al. Effect of Etching and Aging Conditions on the Structural, Chemical and Optical Characteristics of Porous Silicon. Journal of the Korean Physical Society. (2003);42(92):S184-S188.
[11] Asli NA, Yusop SF, Rusop M, et al. Surface and bulk structural properties of nanostructured porous silicon prepared by electrochemical etching at different etching time. Ionics. (2011);17(7): 653–657.
[12] Kumar P, Peter P, Ghosh M, et al. Effect of HF Concentration on Physical and Electronic Properties of Electrochemically Formed Nanoporous Silicon. J Nanomaterials. 2009;2009:7 p.
[13] Young TF, Chen CP. Study on the Si Si Vibrational States of the Near Surface Region of Porous Silicon. Journal of Porous Materials. (2000);7(1-3)339–343.
[14] Vasquez MA, Rodrıguez GA, Salgado GG, et al. FTIR and photoluminescence studies of porous silicon layers oxidized in controlled water vapor conditions. Revista Mexicana De Fisica. (2007);53(6):431-435. [Mexico].
[15] Canaria CA, Lees IN, Wun AW, et al. Characterization of the carbon–silicon stretch in methylated porous silicon – observation of an anomalous isotope shift in the FTIR spectrum. Inorganic Chemistry Communications. (2002);5(8):560–564.
[16] Salcdo WJ, Fernandez FR, Galeazzo E. Structural Characterization of Photoluminescent Porous Silicon with FTIR Spectroscopy. Brazilian J Physics. (1997);27(4):158-161.
[17] Nussupov KK, Beisenkhanov NB [Authors]. Mukherjee M. [Editor]. Silicon Carbide – Materials, Processing and Applications in Electronic Devices, Chapter four. Croatia (HR): InTech; 2011. 558 p.
[18] Pap AE, Kordas K, Vahakangas J, et al. Optical properties of porous silicon. Part III: Comparison of experimental and theoretical results. Optical Materials. (2006);28(5):506–513.

[19] Salman KA, Omar K, Hassan Z. Effective conversion efficiency enhancement of solar cell using ZnO/PS antireflection coating layers. Solar Energy. (2012);86(1):541–547.
[20] Nayef UM. Omnidirectional Mirrors for Porous Silicon Multilayer by Electrochemical Etching. Eng. & Tech. Jornal. (2011);29(15):3185-3193.
[21] Alwan AM, Abd alzahra NZ. The Effect Of Thermal Oxidation Time On The Structure And Influence On Optical Properties For Porous Silicon Prepared By Photo Electrochemical Etching. J Emg. & Tech. (2009);27(4):727-735.
[22] Dzhafarov T [Author]. Acevedo M [Editor]. Solar Cells - Research and Application Perspectives, Chapter Two. Croatia (HR): InTech; (2013). 336 p.
[23] Naderi N, Hashim MR. Effect of Surface Morphology on Electrical Properties of Electrochemically-Etched Porous Silicon Photodetectors. Int. J. Electrochem. Sci. (2012);7(11):11512 – 11518.
[24] Ali NA, Muhammed GS. Study the Effect of Irradiation Time and HF Consentration on Porosity of PS and Study Some of the Electrical Properties of Its Based Device. Advances in Materials Physics and Chemistry. 2012;2:55-58.
[25] Sultan FI, Slman AA, Nayef UM. I-V and C-V Characteristics of Porous Silicon Nanostructures by Electrochemical Etching. Eng. & Tech. Jornal. (2013);31(3):332-338.
[26] Algun G, Arikan MC. An Investigation of Electrical Properties of Porous Silicon. Turkish J Physics. (1999);23(4):789-797.